

EVOLUTION IN THE COLORS OF LYMAN–BREAK GALAXIES FROM $Z \sim 4$ TO $Z \sim 3$ ¹

CASEY PAPOVICH², MARK DICKINSON^{3,4}, HENRY C. FERGUSON^{3,4}, MAURO GIAVALISCO³, JENNIFER LOTZ⁵,
PIERO MADAU⁶, RAFAL IDZI⁴, CLAUDIA KRETCHMER⁴, LEONIDAS A. MOUSTAKAS³, DUILIA F. DE MELLO⁷,
JONATHAN P. GARDNER⁷, MARCIA J. RIEKE², RACHEL S. SOMERVILLE³, AND DANIEL STERN⁸

Accepted for Publication in the Astrophysical Journal Letters

ABSTRACT

The integrated colors of distant galaxies provide a means for interpreting the properties of their stellar content. Here, we use rest-frame UV–to–optical colors to constrain the spectral-energy distributions and stellar populations of color–selected, B –dropout galaxies at $z \sim 4$ in the *Great Observatories Origins Deep Survey*. We combine the ACS data with ground–based near–infrared images, which extend the coverage of galaxies at $z \sim 4$ to the rest–frame B –band. We observe a color–magnitude trend in the rest–frame $m(\text{UV}) - B$ versus B diagram for the $z \sim 4$ galaxies that has a fairly well–defined “blue–envelope”, and is strikingly similar to that of color–selected, U –dropout galaxies at $z \sim 3$. We also find that although the co–moving luminosity density at rest–frame UV wavelengths (1600Å) is roughly comparable at $z \sim 3$ and $z \sim 4$, the luminosity density at rest–frame optical wavelengths increases by about one–third from $z \sim 4$ to $z \sim 3$. Although the star–formation histories of individual galaxies may involve complex and stochastic events, the evolution in the global luminosity density of the UV–bright galaxy population corresponds to an average star–formation history with a star–formation rate that is constant or increasing over these redshifts. This suggests that the evolution in the luminosity density corresponds to an increase in the stellar–mass density of $\gtrsim 33\%$.

Subject headings: early universe — cosmology: observations — galaxies: evolution — galaxies: formation — galaxies: high–redshift — galaxies: photometry

1. INTRODUCTION

Current investigations of high–redshift ($z \gtrsim 2$) galaxies have been focusing on the properties of these objects as a global population. Many surveys identify these galaxies by their strong emission at rest–frame UV wavelengths (observed–frame optical) and spectral breaks at Lyman α and the Lyman limit (so–called Lyman–break galaxies [LBGs]; e.g., Giavalisco 2002). These galaxies are generally dominated by the light from OB stars, and have properties that are similar to local starburst galaxies (e.g., Shapley et al. 2003). Near–infrared (NIR) photometry of galaxies at $z \gtrsim 2$ extends the observations to rest–frame optical wavelengths, probing the light from A– and later–type stars. Several studies have used NIR observations to constrain the properties of the stellar populations of $z \sim 2 - 3$ galaxies (e.g., Sawicki & Yee 1998; Papovich, Dickinson, & Ferguson 2001; Shapley et al. 2001; Labbé et al. 2003; Franx et al. 2003), and to estimate the evolution of the global stellar–mass density for $0 < z \lesssim 3$ (e.g.,

Dickinson et al. 2003).

At present, some of the constraints on the parameters of the galaxies’ stellar–population models are uncertain by more than an order of magnitude (Papovich et al. 2001; Shapley et al. 2001). Even so, the stellar–population ages and star–formation histories of the models have broad implications for galaxy evolution at higher redshifts (see Ferguson, Dickinson, & Papovich 2002). The galaxies’ spectral–energy distributions (SEDs) contain the integrated record of their past and current star formation. Thus, comparing galaxy SEDs at different redshifts allows us to improve the constraints on the star–formation histories of these galaxies.

In this *Letter*, we study galaxies at $z \sim 4$ selected from deep imaging with the Advanced Camera for Surveys (ACS) onboard the *Hubble Space Telescope* (*HST*) and augmented with NIR observations from the ground (§ 2), and we compare these to similar rest–frame colors for color–selected galaxies at $z \sim 3$ from the Hubble Deep Fields, North and South (HDF–N and –S; § 3). We then discuss the SEDs of the luminosity density generated by these galaxies, and we consider the implications on the galaxies’ star–formation histories (§ 4). Throughout this *Letter*, we use a flat cosmology with $\Omega_m = 0.3$, $\Omega_\Lambda = 0.7$, a Hubble constant of $70 \text{ km s}^{-1} \text{ Mpc}^{-1}$, and we use AB magnitudes, $m_{\text{AB}} = -48.6 - 2.5 \log(f_\nu / 1 \text{ erg s}^{-1} \text{ cm}^{-2} \text{ Hz}^{-1})$.

2. THE OBSERVATIONS AND GALAXY SAMPLE

The *HST* data used in this letter stem from the first three epochs of ACS imaging of the Chandra Deep Field South (CDF–S) as part of the Great Observatories Origins Deep Survey (GOODS) program. These data provide imaging in the B_{435} , V_{606} , i_{775} , and z_{850} –bands covering a field of view of $10' \times 16.5'$. The dataset, its reduction procedures, and object cataloging are described in Giavalisco et al. (2003a).

The ACS data only probe rest–frame UV wavelengths for galaxies at $z \gtrsim 1.2$. To study the rest–frame optical light

¹ Based on observations taken with the NASA/ESA Hubble Space Telescope, which is operated by the Association of Universities for Research in Astronomy, Inc. (AURA) under NASA contract NAS5–26555, and based on observations collected at the European Southern Observatory, Chile (ESO Programmes 168.A-0485, 64.O-0643, 66.A-0572, 68.A-0544).

² Steward Observatory, The University of Arizona, 933 North Cherry Avenue, Tucson, AZ 85721; papovich, mrieke@as.arizona.edu

³ Space Telescope Science Institute, 3700 San Martin Drive, Baltimore, MD 21218; med, ferguson, mauro, leonidas, somerville@stsci.edu

⁴ Department of Physics and Astronomy, The Johns Hopkins University, Baltimore, MD 21218; idzi, claudiak@stsci.edu

⁵ Department of Physics, University of California at Santa Cruz, CA 95064; jlotz@scipp.ucsc.edu

⁶ Department of Astronomy and Astrophysics, University of California at Santa Cruz, Santa Cruz, CA 95064; pmadau@ucolick.org

⁷ Laboratory for Astronomy and Solar Physics, Code 681, NASA GSFC, Greenbelt, MD 20771; duilia@ipanema.gsfc.nasa.gov, gardner@harmony.gsfc.nasa.gov

⁸ Jet Propulsion Laboratory, California Institute of Technology, Mail Stop 169-506, Pasadena, CA 91109; stern@zwoolfkinder.jpl.nasa.gov

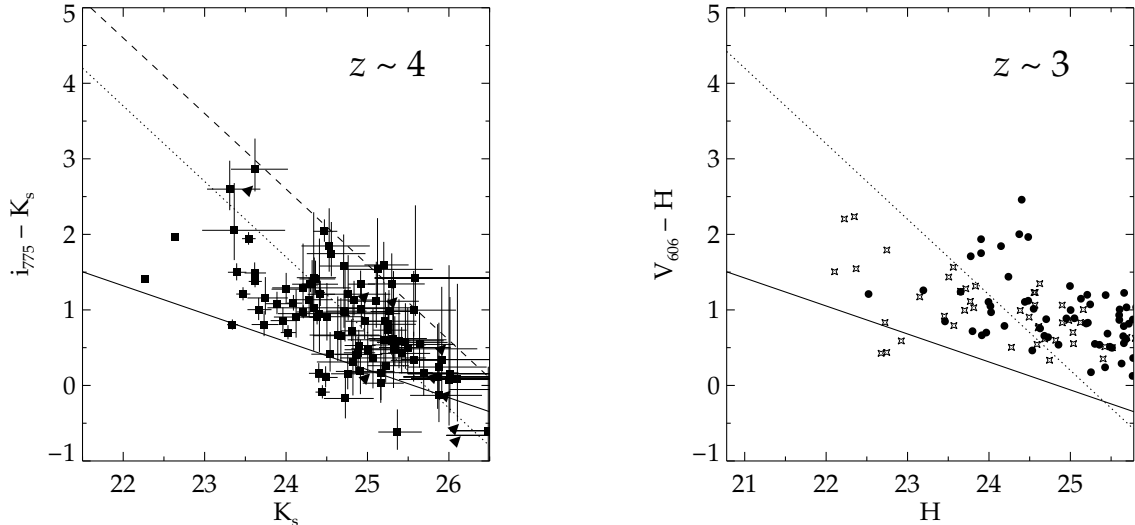


FIG. 1.— Rest-frame UV-optical color-magnitude diagrams for color-selected high-redshift galaxies. *Left*: Panel shows the $i_{775} - K_s$ versus K_s color-magnitude diagram for the B -dropout galaxies selected from the GOODS CDF-S data (*squares*; *triangles* denote 1σ limits). These filters correspond to rest-frame 1600- and 4400-Å colors. The dashed line illustrates the approximate z_{850} -band detection limit (for $i_{775} - z_{850} \approx 0$). *Right*: Panel shows the $V_{606} - H$ versus H color-magnitude diagram for U -dropout galaxies selected from the WFPC2 data for the HDF-N (*filled circles*) and HDF-S (*open stars*). The abscissa of each panel has been adjusted to show an approximately equal range of rest-frame B -band absolute magnitudes. The dotted line shows the magnitude limit ($m^* + 1$ mag) used to define samples that are used to derive the luminosity densities in § 3. The solid line in each panel indicates the fiducial ‘blue-envelope’.

from higher redshift galaxies we combined the ACS data with VLT/ISAAC imaging in the JHK_s bands obtained as part of GOODS (Giavalisco et al. 2003a). Currently, we use eight individual ISAAC tiles covering a total area of 50 arcmin².

We have analyzed the ISAAC JHK_s images to extract optimal photometry matched to the ACS z_{850} -selected catalog. In brief, we use the z_{850} -band data to create two-dimensional templates for each object, convolve these to match the point-spread function (PSF) of the ground-based data, and scale and fit the convolved templates to the JHK_s -band images to extract object fluxes (see C. Papovich et al. *in preparation*; Fernández-Soto, Lanzetta, & Yahil 1999). The advantage of this method as applied to faint galaxies is that it reduces concerns about PSF- and aperture-matching effects on the relative photometry and permits deblending of objects partially merged by the terrestrial seeing.

We identified high-redshift galaxies whose SEDs reveal a spectral discontinuity at the observed Lyman limit, which arises from H I absorption systems along the line of sight (e.g., Madau 1995). We selected “ B -dropout” galaxies with, $B_{435} - V_{606} \geq 1.1 + (V_{606} - z_{850})$, $B_{435} - V_{606} \geq 1.1$, and $V_{606} - z_{850} \leq 1.6$ (see Giavalisco et al. 2003b). Using these colors, we are able to reject most lower-redshift interlopers while detecting galaxies at $z \sim 4$ with bright rest-frame UV spectra (which is indicative of ongoing star formation; Leitherer et al. 1999). Indeed, using the ~ 1400 spectroscopic redshifts available for GOODS objects, we observe no contamination from stars or galaxies at $z < 3$. Our modeling indicates that these criteria identify galaxies with an expected redshift distribution that peaks at $\bar{z} = 3.9$ and tapers to higher and lower redshifts, with 50% completeness limits of $3.4 \lesssim z \lesssim 4.5$.

3. UV-OPTICAL COLORS OF HIGH-REDSHIFT GALAXIES

In the left panel of figure 1, we show the $i_{775} - K_s$ versus K_s color-magnitude diagram for the B -dropout galaxies. For $z \sim 4$, these colors correspond approximately to rest-frame

$m(1600 \text{ \AA}) - m(4400 \text{ \AA})$. Although most of the B -dropout galaxies have relatively blue rest-frame UV-to-optical colors, the brightest galaxies in K_s have redder optical-infrared colors with a fairly well-defined “blue-envelope”. Because this sample is selected in the z_{850} -band, there is no reason to expect that the lack of bright galaxies ($K_s \lesssim 24$) with blue colors is due to some selection effect. At fainter magnitudes, part of this trend may be due to increasing photometric uncertainties. However, the trend among the B -dropouts is apparent even at bright magnitudes where the photometric errors are small, and exists for the U -dropouts (see below), where the optical and IR data are much deeper than the GOODS data.

A similar blue-envelope exists for the colors of galaxies at $z \sim 3$. The right panel of figure 1 shows the $V_{606} - H$ versus H -band color-magnitude diagram for U -dropout galaxies from the WFPC2 and NICMOS data of the HDF-N (Papovich et al. 2001; M. Dickinson et al. *in preparation*) and from the WFPC2 and VLT/ISAAC data of the HDF-S (Labbé et al. 2003), and using the color-selection of Steidel et al. (1999). The U -dropout criteria identify galaxies with a mean redshift, $\bar{z} \approx 2.6$, and 50% completeness limits of $2.0 \lesssim z \lesssim 3.3$. Although the galaxy samples for the HDF-N and -S are originally detected in NIR data, our tests using an I -band-selected sample for the HDF-N yield essentially no change in the number of selected U -dropout galaxies nor in the number and luminosity densities derived below. The advantage of using these data is that they provide band-matched catalogs from optical-to-NIR wavelengths that are comparable to the data for the B -dropout galaxies.

For the $z \sim 3$ galaxies, the $V_{606} - H$ color corresponds to nearly identical rest-frame colors as $i_{775} - K_s$ for the galaxies at $z \sim 4$. The color-magnitude trends at $z \sim 3$ and 4 are strikingly similar. Thus, the LBGs at both $z \sim 3$ and $z \sim 4$ seem to require that either (or likely some combination of) the mean stellar population age, metallicity, and/or dust opacity increase with optical luminosity. Furthermore, we also note

that the U -dropout galaxies have slightly redder rest-frame $m(1600\text{\AA})-m(4400\text{\AA})$ colors as evidenced by the fact that the “blue-envelope” shifts by ~ 0.2 mag. This reddening seems to imply that the mean ages, metallicity, and/or dust opacity are actually increasing from $z \sim 4$ to 3.

4. THE INTEGRATED SEDS OF HIGH-REDSHIFT GALAXIES

To measure the number and luminosity densities, we require the redshift distribution and effective volumes probed by the U - and B -dropout criteria. For the U -dropout galaxies, we have used the effective volume derived by Steidel et al. (1999). For the B -dropout galaxies, we have simulated artificial LBGs in the GOODS data with a distribution of colors and sizes that match the observed B -dropout properties (see Ferguson et al. 2003). We then measure photometry for the simulated galaxies and apply our color-selection criteria to derive the probability that a LBG with given magnitude and redshift is detected in the data, $p(m, z)$. This technique accounts for incompleteness due to magnitude and surface-brightness effects as well as the color-selection process. We then compute the effective volumes, $V_{\text{eff}}(m) = \int dz p(m, z) dV(z)/dz$. Because these selection criteria are insensitive to heavily obscured galaxies and to galaxies with passively evolving, older stellar populations, our estimates of galaxy densities are strictly lower limits, derived from the UV-bright population alone.

To calculate the galaxy densities we consider galaxies brighter than $m^* + 1$ mag, where $m^*(\mathcal{R}) = 24.20$ for the U -dropouts (Steidel et al. 1999; where $\mathcal{R} \approx (V_{606} + I_{814})/2$, and m^* has been adjusted slightly to account for differences in cosmology and the mean redshifts of the samples here and those of Steidel et al.), and $m^*(I) = 24.70$ for the B -dropouts (Giavalisco et al. 2003b). We derive specific luminosity densities by integrating the flux densities in each bandpass to $m^* + 1$ mag (where the B -dropout galaxies are well-detected in both the ACS and ISAAC data, see figure 1): $\rho_\nu = \int dL_\nu(m) n(m) L_\nu(m) / V_{\text{eff}}(m)$, where $n(m)$ is the observed number density, $L_\nu(m) = 10^{-0.4(48.6+m)} 4\pi d_L^2 (1+z)^{-1}$, and d_L is the luminosity distance. We plot the measured values in figure 2 along with uncertainties from a bootstrap resampling. Note that we have made no correction for fainter galaxies.

The area of the HDFs and the portion of the GOODS field with ISAAC imaging are fairly small, and cosmic variance may be a substantial source of uncertainty (see Somerville et al. 2003). To limit this effect on our results, we have normalized the luminosity densities of both the U - and B -dropout samples such that they match the rest-frame UV values of Steidel et al. (1999) and Giavalisco et al. (2003b), respectively, while preserving the measured “color” between the rest-frame UV and other wavelengths. These surveys average over more area and sightlines than considered here, which significantly reduces the uncertainties from cosmic variance. Cosmic variance may still be a factor for the B -band luminosity densities. The luminosity weighted mean rest-frame $m(1600\text{\AA})-m(4400\text{\AA})$ colors of the U -dropout galaxies in the HDF-N and -S vary by $\simeq 0.15$ mag, which provides an estimate on the uncertainty in the typical luminosity-density colors of LBGs in single HDF-sized fields. Future studies using the entire GOODS dataset (with full U -band and NIR observations of both fields) will substantially increase the sample size of both the U - and B -dropouts by roughly a factor of ≈ 25 and 10, respectively, and should strengthen our results.

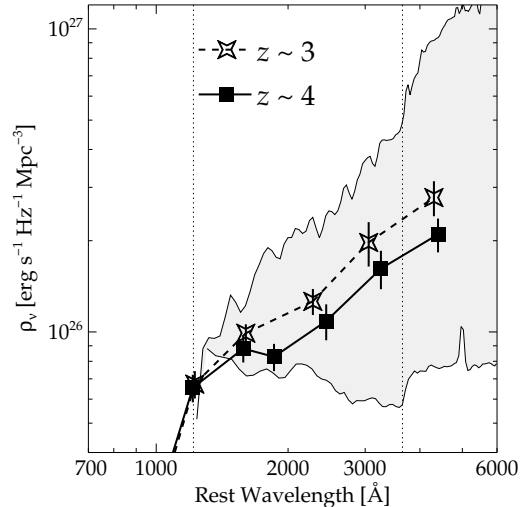


FIG. 2.— The co-moving luminosity density as a function of rest-frame wavelength. The data points show the values derived for the B -dropout galaxies in the GOODS CDF-S data (filled squares, solid lines) and for the U -dropouts in the HDF-N and S (open stars, dashed lines). The luminosity densities have been integrated down to $m^* + 1$ mag with no correction for galaxies fainter than this limit or due to dust extinction (see text). The shaded region spans the range of empirical starburst galaxy SEDs from Kinney et al. (1996), from the bluest [NGC 1705, $E(B-V) \simeq 0.0$] to reddest [$0.6 < E(B-V) < 0.7$] templates. The vertical dotted lines indicate Lyman α and the Balmer Break.

The fact that the rest-frame 1600 \AA luminosity density is roughly unchanged (to within $\lesssim 10\%$) implies that the star-formation rate (SFR; at least of massive, OB stars) is roughly constant (see, e.g., Madau, Pozzetti, & Dickinson 1998). However, we observe marginal evidence for a steepening of the UV continuum ($\sim 1500-2500$ \AA), and strong evidence ($\approx 98\%$ confidence) that the average $m(1600\text{\AA})-m(4400\text{\AA})$ color becomes redder for the U -dropouts relative to those for the B -dropouts. In particular, the luminosity density at rest-frame 4400 \AA grows from $2.1 \pm 0.3 \times 10^{26}$ $\text{erg s}^{-1} \text{Hz}^{-1} \text{Mpc}^{-3}$ at $z \sim 4$ to $2.8 \pm 0.3 \times 10^{26}$ $\text{erg s}^{-1} \text{Hz}^{-1} \text{Mpc}^{-3}$ at $z \sim 3$. Based on the observed color distribution of LBGs (to fainter magnitude limits than our samples here), our simulations suggest that this result is unlikely to be biased significantly by the color-selection of these galaxies. This change in the mean color suggests that the mean stellar mass-to-light ratio of these galaxies is also increasing. Therefore, the total stellar mass density of this population is presumably growing by more than the $\gtrsim 33\%$ increase seen in the rest-frame B -band optical light. Dickinson et al. (2003) found evidence for a substantial build-up in the global stellar mass density from $z \sim 3$ to $z \sim 1$. The present results extend that trend to still higher redshifts.

The luminosity densities constrain the global, average star-formation histories of galaxies at $z \sim 3-4$. One possible scenario is a roughly constant SFR with an unchanging dust content. This would produce approximately equal $\rho_\nu(1600\text{\AA})$ at $z \sim 3$ and 4, and build up the global stellar mass with time, which would redden the average galaxy SED from $z \sim 4$ to $z \sim 3$ as the B -band light increases. We note that the Universe ages by $\sim 50\%$ from $z \sim 4$ to 3, and may imply that galaxies formed stars at a near-constant rate from $z \gg 6$ to 3. An alternative scenario is a rising SFR from $z \sim 4$ to 3 with an

increasing dust content that is tuned to produce a roughly constant $\rho_\nu(1600\text{\AA})$, and is consistent with the suggestion that the UV continuum is redder at $z \sim 3$. The fractional stellar-mass build-up in this scenario would be still greater than that with constant SFR and an unchanging dust content.

Both of the above scenarios invoke a SFR that is either constant or growing in time. However, the stellar populations observed in $z \sim 3$ galaxies appear to be young (a few $\times 10^8$ yr for simple, monotonic star-formation histories; Sawicki & Yee 1998; Papovich et al. 2001; Shapley et al. 2001), which implies that these stars had not formed by $z \sim 4$. Galaxies at these redshifts probably have star-formation histories that are more complex (with multiple formation episodes) than those described by the simple models (see Ferguson et al. 2002). However, even though the star-formation histories for individual galaxies may be fairly stochastic, the global, average SFR at high redshift must be roughly constant in order to explain the evolution in the UV and optical luminosity densities.

Although the increase in the observed optical luminosity density from $z \sim 4$ to $z \sim 3$ appears robust, the uncertainties due to cosmic variance and other systematics are non-negligible. If there is, in fact, no evolution in the optical luminosity density then this could imply that stars formed in the B -dropout galaxies are not present within the U -dropout galaxies, and that at some point the $z \sim 4$ galaxies cease forming stars and evolve beyond the U -dropout selection criteria. This would have interesting implications for constraints on the sources of reionization and/or on the IMF at higher redshifts (see, e.g., Ferguson et al. 2002). However, this would likely be inconsistent with the low number density of red, $z \gtrsim 2$ objects (Franx et al. 2003). Moreover, the majority of galaxy evolution models predict growth in the stellar-mass density by amounts consistent with our observations (although specific predictions vary from model to model; see Dickinson et al. 2003, and references within), and this suggests that much of the stellar-mass assembly at high-redshifts does occur in these UV-bright galaxies.

5. SUMMARY

We have compared the rest-frame UV-optical colors of color-selected galaxies at $z \sim 4$ to those of similarly selected

galaxies at $z \sim 3$. We find a great degree of similarity in the rest-frame $m(\text{UV}) - B$ versus B diagram for galaxies from $z \sim 3 - 4$. However, although the rest-frame UV luminosity densities at $z \sim 4$ and $z \sim 3$ are comparable, there is evidence that the rest-frame B -band luminosity density grows by $\approx 33 \pm 16\%$. Even though the star-formation histories of individual galaxies may involve complex and stochastic processes, the evolution of the luminosity density corresponds to a globally average SFR that is constant or increases with time. This implies that the average stellar-mass-to-light ratio of galaxies is also increasing over this redshift range and that the global stellar-mass density grows by more than $\gtrsim 33\%$ over the ~ 1 Gyr interval that elapses between $z \sim 4$ and 3.

By selecting in the rest-frame UV, we are likely to miss galaxies without ongoing, relatively unobscured star formation. For example, Franx et al. (2003) have used deep NIR images of the HDF-S to identify red galaxies which may have evolved, massive stellar populations at $z \sim 2$, and may contribute significantly to the global stellar mass density. Such objects would be missing from the samples here, leading to an underestimate of the total density. Logically, the number and mass content of these red galaxies should grow as the Universe ages. Therefore, the apparent increase in stellar mass density from $z \sim 4$ to 3, as traced here by the UV-bright population, would only be strengthened if red, UV-faint objects were also considered. Ultimately, the full GOODS dataset will permit more direct tests of the star-formation histories of the distant galaxy population, as will future observations with the *Space Infrared Telescope Facility* and the *James Webb Space Telescope*.

We wish to thank our colleagues for stimulating conversations, and the entire GOODS team for their concerted effort. Support was provided by NASA through grant GO09583.01-96A from STScI, which is operated by the AURA, under NASA contract NAS 5-26555. Support for this work, part of the *SIRTf* Legacy Science Program, was provided by NASA through Contract Number 1224666 issued by the Jet Propulsion Laboratory, under NASA contract 1407. PM acknowledges support by NASA through grant NAG5-11513.

REFERENCES

- Calzetti, D., Armus, L., Bohlin, R. C., Kinney, A. L., Koornneef, J., & Storchi-Bergmann, R. 2000, *ApJ*, 533, 682
 Dickinson, M., Papovich, C., Ferguson, H. C., & Budavári, T. 2003, *ApJ*, 587, 25
 Fernández-Soto, A., Lanzetta, K. M., & Yahil, A. 1999, *ApJ*, 513, 34
 Ferguson, H. C., Dickinson, M., & Papovich, C. 2002, *ApJ*, 569, L65
 Ferguson, H. C., et al. 2003, *ApJ*, in press (astro-ph/0309058)
 Franx, M. et al. 2003, *ApJ*, 587, L79
 Giavalisco, M. 2002, *ARA&A*, 40, 579
 Giavalisco, M. et al. 2003a, *ApJ*, in press (astro-ph/0309105)
 Giavalisco, M. et al. 2003b, *ApJ*, in press (astro-ph/0309065)
 Kinney, A. L., Calzetti, D., Bohlin, R. C., McQuade, K., Storchi-Bergmann, T., & Schmitt, H. R. 1996, *ApJ*, 467, 38
 Labbé, I. et al. 2003, *AJ*, 125, 1107
 Leitherer, C. et al. 1999, *ApJS*, 123, 3
 Madau, P. 1995, *ApJ*, 441, 18
 Madau, P., Pozzetti, L., & Dickinson, M. 1998, *ApJ*, 498, 106
 Papovich, C., Dickinson, M., & Ferguson, H. C. 2001, *ApJ*, 559, 620
 Sawicki, M., & Yee, H. K. C. 1998, *AJ*, 115, 1329
 Shapley, A. E., Steidel, C. C., Adelberger, K. L., Dickinson, M., Giavalisco, M., & Pettini, M. 2001, *ApJ*, 562, 95
 Shapley, A. E., Steidel, C. C., Pettini, M., & Adelberger, K. L. 2003, *ApJ*, 588, 65
 Somerville, R. S., Lee, K., Ferguson, H. C., Gardner, J. P., Moustakas, L. A., Giavalisco, M., & Renzini, A. 2003, *ApJ*, in press (astro-ph/0309071)
 Steidel, C. C., Adelberger, K. L., Giavalisco, M., Dickinson, M., & Pettini, M. 1999, *ApJ*, 519, 1